Geotechnical Engineering Journal of the SEAGS & AGSSEA Vol. 42 No. 4 December 2011 ISSN 0046-5828

Development of a hollow cylinder torsional apparatus for pre-failure deformation and large strains behaviour of sand

E**.** Ibraim, P. Christiaens and M. Pope
Department of Civil Engineering, University of Bristol, Bristol, UK
E-mail: erdin.ibraim@bris.ac.uk

ABSTRACT: A hollow cylindrical torsional apparatus (HCTA) recently developed at University of Bristol, UK is presented. The HCTA apparatus is testing granular soils in drained and undrained, in monotonic but also dynamic loading conditions, and it is equipped with a complex strain measurement system based on high resolution non-contact transducers. The experimental developments are designed to allow the study of the pre-failure deformation characteristics and the large strains behaviour, via a continuous test on a single specimen and, thus, analyse the soil stiffness with the evolution of the strain and stress levels. While the experimental developments and apparatus capabilities in large strains have been explored and validated in an earlier study, this paper describes mainly the precision measurement system, including the assessment of its performance with reference to the soil stiffness.

1. INTRODUCTION

Rotation of principal axes of stress or strain occurs in practice under most types of loading (Arthur et al., 1980) and, knowing the anisotropic nature of strength and deformation characteristics of soils, this cannot be ignored. One approach to study in laboratory the effect of principal stress or strain rotation is to apply to a cylindrical sample simultaneously a combined axial and torsional loads (or axial and shear strains) so that the induced shear stress will cause the principal stress to rotate from the vertical direction. There is however an inevitable radial variation of stresses and of strains and this can be minimized via a thin wall hollow cylindrical sample. A Hollow Cylinder Torsional Apparatus (HCTA) can therefore control four degree of external freedom including all three principal stresses and the rotation of one set of principal axes.

In most geotechnical problems, excluding particularly deformable soils such as soft clays or loose sands, the operational strain domain ranges from very small to medium, less than around 10^{-3} m/m (Jardine et al., 1986). Advanced numerical analysis can be used to predict serviceability response of geotechnical systems. However, owing to the complexity of the soil behavior in this range of strains, realistic prediction of ground deformations and geotechnical structural displacements is only possible if the constitutive models of soil deformation and stiffness – essential ingredients of any numerical analysis – are supported by relatively sophisticated soil laboratory testing and data (Clayton, 2010).

In the laboratory the measurement of stiffness of soils in the small strain domain can be achieved using the following three methods: the resonant column test (Hardin and Richart, 1963, Hardin and Black, 1966), the measurements of the body wave velocities within the soil element (Shirley and Hampton, 1978, Schultheiss, 1980, Dyvik and Madshus, 1985, Viggiani and Atkinson, 1995, Brignoli et al., 1996, Pennington et al., 1997, Cazacliu and Di Benedetto, 1998, Yamashita et al., 2009) and the direct measurement of small strain and stress amplitudes during monotonic or cyclic quasi-static loading - dependent on very accurate and reliable measuring transducers. While the first two methods present real challenges in data interpretation (Arroyo et al., 2006, Clayton et al., 2009) based on the theory of wave propagation and require either prior knowledge of a constitutive model for soil or manipulation of continuum medium theory assumptions, the latter has the advantage of giving direct access to the stiffness of the soils providing that the measurement system is capable of removing the measurement errors.

Jardine et al. (1984) and Baldi et al. (1988) identify the potential measurement errors induced by insufficient precision, accuracy of the sensors and data acquisition, compliance of loading system and misalignment, sample bedding/seating effects. It is also widely recognized that the stiffness of sand, evaluated with traditional external strain measurements is smaller than that determined by measurements in the central part of the sample (Shibuya et al., 1992, Tatsuoka et al., 1994). At the same time, it is a desirable requirement of soil laboratory investigation to be able to study the pre-failure deformation characteristics and the large strain behaviour, up to 15×10^{-2} m/m, using a continuous test on a single soil sample. That is, to analyze the soil stiffness with the evolution of the strain and stress levels (Tatsuoka et al., 1998). In these conditions, any development of local strain measurement system, especially for a HCTA, represents a real technical challenge. If the type of the transducer (Linear Variable Differential Transformer (LVDT), Hall Effect, non-contact, Local Deformation Transducers (LDT), for example) could drive the specific design of the mounting system, the balance between the necessary sensor resolution and its measurement range could often require the re-positioning of the sensors during the tests. In addition, the mounting system should accommodate coupled tri-dimensional displacements and the development of inevitable sample non-uniformities. Several types of torsional shear apparatus have been developed in order to have access to pre-failure characteristics of soils under conditions of rotating principal axes (Hight et al., 1983, Lo Presti et al., 1993, Zdravkovic and Jardine, 1997, Connolly and Kuwano, 1999, Chaudhary et al., 2004, O'Kelly and Naughton, 2005). The most complex measurement systems for torsional hollow cylindrical apparatus use non-contact sensors and bender elements (Cazacliu and Di Benedetto, 1998) and LDTs and non-contact transducers (HongNam and Koseki, 2003).

A new hollow cylindrical torsional apparatus was recently developed at the Department of Civil Engineering, University of Bristol, UK. The HCTA apparatus is testing granular soils in drained and undrained, in monotonic but also dynamic loading conditions, and it is equipped with a complex strain measurement system based on high resolution non-contact sensors designed to provide access to the soil stiffness, including its evolution with the general strain and stress levels. While the general apparatus capabilities including large strain behaviour have been explored and validated through a preliminary work conducted on sand by Boung Shik (2005), this paper is concentrating on the description of the precision strain measurement system, the assessment of its performance and validation through some basic testing loading conditions.

2. HOLLOW CYLINDRICAL TORSIONAL APPARATUS

2.1 General description

The HCTA consists of a 200ℓ confining cell fitted with internal tie bars. An overall view of the apparatus is given in Fig. 1. Any cell pressure up to 800kPa can be safely employed. The apparatus can test samples with an outside diameter of 100mm, 20mm wall thickness and 200mm height. The degree of stress and strain non-uniformities, inevitable as a result of the sample curvature and the restraint at its ends, is directly related to the sample dimensions. Sayao and Vaid (1991) suggested the following desirable

dimensions of the hollow cylindrical sample: (i) wall thickness between 20 and 26 mm; (ii) ratio of inner to outer radius ranging between 0.65 and 0.82; (iii) ratio of height to outer diameter from 1.8 to 2.2. Our sample dimensions satisfy the first and third condition, while for the second one the ratio of inner to outer radius is 0.6, close to the lower limit.

Figure 1 Overall view of the HCTA.

Compared with an average value, the shear strain across the wall varies between ± e/D, where e is the wall thickness and D is the average diameter. A low ratio of wall thickness to diameter would increase the uniformity of the shear strain, but would also increase the gradient of radial stress if internal and external pressures are not the same. A compromise was necessary.

2.2 Loading system

The apparatus has the benefit of two independent axial (compression/extension)/rotational loading systems: one hydraulic (two actuators located on the top of the cell) and the other one pneumatic (frictionless air cylinders - Bellofram model – located on the bottom of the cell). Three servo hydraulic cells are also available for the control of the inner cell pressure, p_i, outer cell pressure, p_o, and u, the pore water pressure in the sample. In addition, an independent pneumatic pressurising system for p_i, p_o, and u, is accessible through a control panel fitted with a set of very accurate manual pressure regulators, three air/water interface cells, and three pressure gauges. The control system is fitted with appropriate connections to allow the control of either equal or different inner cell/outer pressures, but also to assist as appropriately the change between the hydraulic and pneumatic pressure loading systems. The use of the hydraulic system is required for cyclic/dynamic soil investigations (high quality control for frequencies up to 20Hz) and is essential for the small strain soil investigation as any change of the loading direction needs to be virtually backlash free. In this study, the axial/rotational hydraulic system was employed for monotonic and quasi-static cyclic loadings while the control of the inner/outer cell and pore pressures was done manually by using the pneumatic system.

2.3 Overall sample measurement system

The HCTA is fitted with a submersible combined force/torque load cell with 8kN/400Nm capacity placed inside the confining cell, at the top of the specimen to eliminate the effects of parasitic ram friction. For a very dense sample, no more than 400kPa of effective cell confining stress can be employed. The overall axial and shear strain measurements are provided by a LVDTs (Linear Variable Differential Transformers) and a RCDT (Rotary Capacitive Displacement Transducer), respectively. Both transducers are located outside the pressurising cell, and fixed either above or below the cell depending on the axial/rotational loading type system employed - hydraulic or pneumatic. Two identical volume change devices are also used, one for the measurement of the overall sample volume, and the other one for the inner cell variations. The two volume change measurements, corrected for the membrane penetration effects and combined with the height variations given by the LVDTs, allow the calculation of the radial (inner and outer) specimen displacements. Three pressure transducers for continuous recording of the inner cell, p_i, outer cell, p_o, and pore water, u, pressures also equip the HCTA. In order to limit the errors in the measurement of the volume changes and pore pressures, a drainage system with minimum length and very stiff tubes and valves without volume variations were installed. Assessment of transducers resolution, long-term stability, calibration characteristics and experimental procedures are given by Boung Shik (2005).

2.4 Control system

The axial and rotational pneumatic loading provided by the frictionless Bellofram air cylinders are digitally controlled by a pair of manostat units with a minimum pressure change increment of 0.1kPa. A third manostat unit can be used for the control of the inner and outer sample confining pressures but these pressures can also be manually controlled through pressure regulators. A 16 channels Datascan analogue/digital unit with 16 bits resolution and adapted data acquisition software complet the pneumatic control system.

The control of the hydraulic system for the axial force, torque, and pressures p_i, p_o, and u is done by a central five axes Instron controller unit that integrates GPIB and PCI cards and a 16 channels analogue/digital data acquisition system with a 19 bits resolution. The data acquisition and control is based on an Instron built in software and a LabVIEW programme as specific interface for soil mechanics stress and strain control (or related variables). The latter is in progress of upgrading thus responding specific needs for application and control of complex stress/strain paths.

3. SMALL STRAIN STIFFNESS

3.1 Small strain domain

As precision of strain measurement of soil samples has spectacularly improved over the last two-three decades, it has become clear that the region of stress or strain in which soils might be described as perfectly elastic is very small corresponding to strain levels of the order of 10^{-8}-10^{-6} m/m (Y1 boundary region in the stress space, Jardine, 1992, Tatsuoka and Shibuya, 1992). As the strain level increases beyond the elastic zone the soil stiffness falls off rapidly (Lo Presti et al., 1997, Clayton and Heymann, 2001). Deformation and strength characteristics of most soils are usually not isotropic: the elastic properties depend on the orientation of the co-ordinate axes to which the properties are referred and the material is said to be anisotropic. Anisotropy (and its description) is important because of the effect that it has an attracting stress, on propagation of shear waves and on the seismic response of granular materials (Simpson et al., 1996). Therefore, there is a real need for complete studies on the soil stiffness and inherent and stress-induced stiffness anisotropy in more complex stress conditions.

3.2 Compliance matrix

For a linear elastic material, the relationship between strain, $[\varepsilon^e_{ij}]$ and effective stress tensors, $[\sigma'_{kl}]$, is described by the equation: $[\varepsilon^e_{ij}] = [C^e_{ijkl}]\,[\sigma'_{kl}]$, where $[C^e_{ijkl}]$ is the stress state-independent elastic compliance matrix. For a hypoelastic material, this constitutive equation is valid only in terms of stress and strain increments, and takes the form: $[d\varepsilon^e_{ij}] = [(C_1)^e_{ijkl}]\,[d\sigma'_{kl}]$, where $[(C_1)^e_{ijkl}]$ is assumed to be symmetrical and independent of the effective stress increment path (provided the stress increments are sufficiently small), but dependent on stress state or stress history. For an isotropic material, only two elastic constants, Young's modulus (E) and Poisson's ratio (ν) are required to describe the terms of the compliance matrix. However, a general description of an anisotropic elastic material requires 36 independent parameters, which become 21 with the assumption of a symmetrical compliance matrix or 9 for orthotropic behaviour. As many soils deposited naturally or in artificial

conditions exhibit cross-anisotropic deformation properties, which are symmetrical about the vertical axis. Cross-anisotropy requires only five independent elastic parameters for the characterisation of soil properties, E_v, E_h, ν_{vh}, ν_{hh} and G_{vh}, where 'v', 'h' and G represent, respectively, the vertical direction, the horizontal directions and the shear modulus. Even for this latter model, only limited experimental data are available for the full compliance matrix $[(C_1)^e_{ijkl}]$ (Bellotti et al., 1996, Fioravante, 2000, Lings et al., 2000, Chaudhary et al., 2004, Kuwano and Jardine, 2002, Duttine et al., 2007).

Recently, two hypoelastic models, DBGS (Di Benedetto et al., 2001, Geoffroy et al., 2003) and IIS (HongNam and Koseki, 2005) have been developed to simulate the stress-induced anisotropy of quasi-elastic deformation properties of sand, with and without rotation of principal stress axes. The latter model takes also into account the effects of inherent anisotropy. Both studies - using torsional hollow cylinder apparatus and sand specimens, and following different stress paths - conducted experimental investigations of some terms of the 4x4 $[C^{eq}]$ equivalent incremental compliance matrix of $[d\varepsilon] = [C^{eq}]\,[d\sigma']$ constitutive equation and with:

$$\begin{bmatrix} d\varepsilon_r^{sa} \\ d\varepsilon_\theta^{sa} \\ d\varepsilon_z^{sa} \\ d\gamma_{z\theta}^{sa}/\sqrt{2} \end{bmatrix} = \begin{bmatrix} \frac{1}{E_r} & -\frac{\upsilon_{\theta r}}{E_\theta} & -\frac{\upsilon_{zr}}{E_z} & 0 \\ -\frac{\upsilon_{r\theta}}{E_r} & \frac{1}{E_\theta} & -\frac{\upsilon_{z\theta}}{E_z} & 0 \\ -\frac{\upsilon_{rz}}{E_r} & -\frac{\upsilon_{\theta z}}{E_\theta} & \frac{1}{E_z} & 0 \\ 0 & 0 & 0 & \frac{1}{2G_{z\theta}} \end{bmatrix} \begin{bmatrix} d\sigma_r^{sa} \\ d\sigma_\theta^{sa} \\ d\sigma_z^{sa} \\ d\tau_{z\theta}^{sa}\sqrt{2} \end{bmatrix} \quad (1)$$

where γ represents the shear strain, the subscripts 'r, θ, z' the cylindrical references, while the superscript 'sa' means 'single amplitude' which is taken as the half of double amplitude of quasi-static cyclic stresses and strains. The experimental results on sand show that this equivalent matrix seems to be independent of the loading direction and relatively constant in the very small strain domain, lower than $2\text{-}3\text{x}10^{-5}$. A limit compliance matrix could be defined in this small strain domain.

3.3 Small strain measurement system

A general view of the local system of measurement of strains developed for the new hollow cylinder torsional apparatus is shown in Figure 2. Six non-contact displacement $\mu\varepsilon$ transducers (based on eddy current effect) with a measurement range of 2mm have been selected for their excellent technical qualities: resolution, linearity, long-term stability, and waterproof. A typical time-response of a $\mu\varepsilon$ transducer shows a resolution better than 0.1μm (Figure 3).

The vertical and circumferential displacements are measured in the central part of the specimen using two pairs of non-contact transducers fixed on stainless steel rods. The corresponding rectangular aluminium plate targets are fixed at different locations on the outer side of the sample, as schematically shown in Figures 4a and 4b. The outer radial sample displacements are deduced by the average of the measurements given by two non-contact transducers pointing aluminium foil targets placed on the sample's side of the outer membrane - in direct contact with the sand (Figure 4c). A specific study by Ibraim (1993) showed that the measurements performed by this type of transducers are not influenced by the presence of the membrane between the sensor and the target, the penetration of the target (aluminium foil) by the sand grains or by the slight rotations of the target relative to the sensor. While one LVDT, positioned as shown in Figure 4c, can be used for direct measurements of the inner radial sample displacements, in this study, the current inner radius changes have been calculated from the volume changes of the inner cell (corrected for the membrane penetration effects) combined with the vertical sample variations.

A common test procedure for small strain and evolution of the quasi-elastic properties corresponds to the repetition of two stages applied at different levels of the stress path (Figure 5). First, a monotonic loading (axial compression or extension, torque) brings the specimen to a deformed state, 1,..i,..n. Second, at this state, called the investigation point, the behaviour of the specimen in the small strain domain is studied by application of a quasi-static cyclic loading of small amplitude. This step is repeated up to large strains. Technically, the resolution of a non-contact transducer is increasing with the decrease of its measurement range. In order to take advantage of this high resolution over a complete test and up to large strains, the non-contact transducers have to be re-located during a complete test, so the best accuracy for strains is maintained at each investigation point 1,..i,..n. Therefore, complex technical solutions have been developed in this case for each pair of the non-contact transducers in order to allow the adjustment of their position from outside the confining cell.

Figure 2 Local small strain measurement systems.

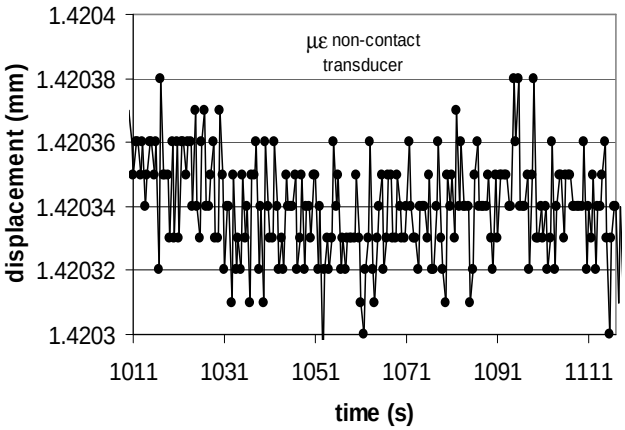

Figure 3 Typical output of a non-contact $\mu\varepsilon$ sensor.

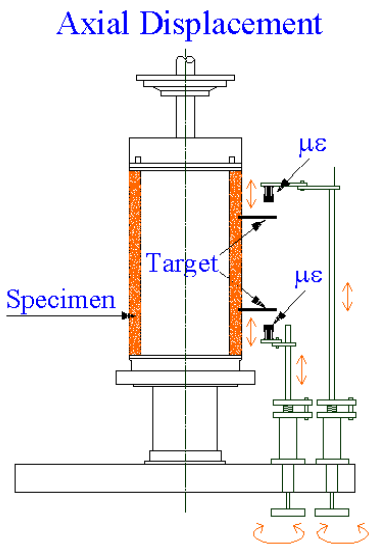

(a)

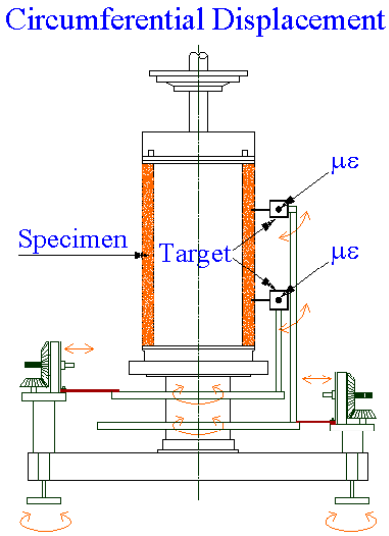

(b)

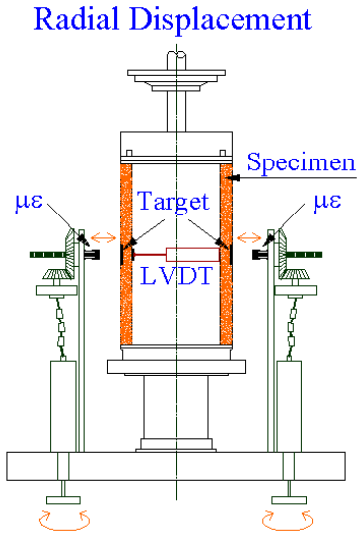

(c)

Figure 4 Schematic view of the mounting systems of the high resolution με transducers

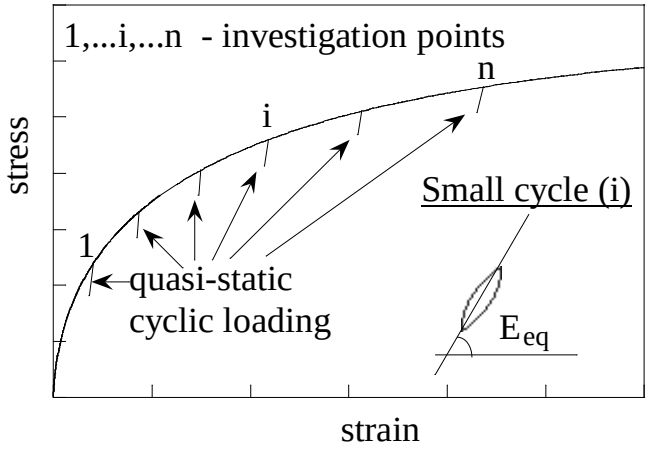

Figure 5 Typical test: large strains and small cycles in different investigation points 1, i, n

In principle, the rotational movement of the drive shaft which passes through the bottom of the cell plate is transformed by a system of bevel gears into horizontal, vertical or circumferential transducer displacements (Figure 4). Preliminary calibration tests showed that the mounting systems respond well under pressure and submerged conditions: while the re-positioning of the transducers is done with minimal effort, once the new position is reached, the transducers are fully fixed and system does not allow any parasitic movements to occur. In addition, no water leaks at the bottom of the cell or pressure cell drops have been observed. At each investigation point, small quasi-static unload/reload cycles can then be performed and thus explore the amount of reversibility along different stress and strain paths. Appropriate control of stresses allows determination of various elements of the compliance matrix, $[C^{eq}]$ (1).

It is well known that the inaccuracies on the values of the variables measured with transducers are induced by a series of random errors normally due to: (i) the electric signal output of the transducer and to the resolution of data acquisition unit (noise, hysteresis, repeatability); (ii) the sensitivity of the sensors: linearity of the calibration curve, measurement of the calibration factor, accuracy of the calibration device; (iii) the validity of the postulated hypothesis of homogeneous strain field development during the test; (iv) the accuracy of the measurement of the initial sample size. During repeated measurements of a given variable δ, these random errors lead to a scatter of measurements around a mean value m_δ. An indication of this scatter is given by the standard deviation σ_δ, which represents the precision of the measured variable δ. The full derivation of the mean and standard deviation of the variables δ of the HCTA high precision transducers based on the method of central moments was given by Palomero (2002) and Christiaens (2006). Based on these values, it was then possible to estimate the theoretical precisions with which the strains could be calculated: $2x10^{-6}$ for axial strain, ε_z, $5x10^{-6}$ for radial strain, ε_r, 10^{-7} for circumferential strain, ε_θ, and 10^{-6} for shear strain, γ.

4. EXPERIMENTAL RESULTS AND VALIDATION

A first series of preliminary test has been performed on dry Hostun RF (S28) sand samples prepared by air pluviation through a funnel with zero height of fall of sand (Christiaens, 2006).

The grain size distribution of the Hostun RF (S28) sand is shown in Figure 6 while its physical characteristics are: mean grain size, D_{50} = 0.38mm, coefficient of uniformity, $C_u = D_{60}/D_{10} = 1.9$, coefficient of gradation, $C_g = (D_{30})^2/(D_{10}D_{60}) = 0.97$, maximum and minimum void ratio, $e_{max} = 1.041$, $e_{min} = 0.648$, and specific gravity $G_s = 2.65$.

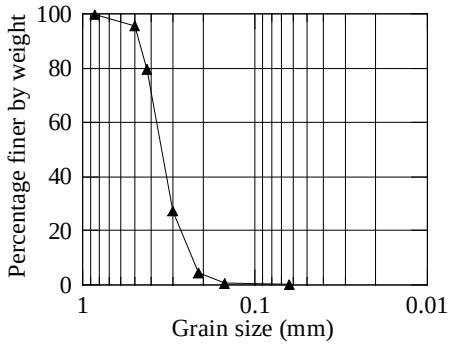

Figure 6 Grain size distribution of Hostun RF (S28) sand

These preliminary tests allowed the assessment of the response of the non-contact transducers including small mechanical adjustments to the mounting systems, procedures and solutions for the fixing of the local measurement targets for axial and circumferential displacements. The targets consisted initially of individual aluminium plates directly attached to the specimen's wall with the aid of two pins of 0.5 mm diameter pushed through the membrane into the sand specimen. The transducers response showed that this solution does not provide a good fixity of the target and subsequently was replaced by setting up the targets on two aluminum rings, each ring being attached on the outer membrane (Figure 7) on three points through flexible suspension connections, as initially proposed by Di Benedetto et al. (2001).

Figure 7 Aluminum targets fixed on two rings located on the central part of the specimen (top and bottom); the flexible suspension connections are glued on the outer membrane

Figure 8 shows the initial response of a dry sand sample (initial void ratio, e_o=0.755) subjected to a triaxial compression loading at a confining stress of 78 kPa. The relationship between the deviator stress and the locally measured axial strain at small strains less than 2-3x10^{-5} is quasi-linear while for the external measure (outside the confining cell) there is no separation between the displacement of the sample and the compliance and bedding errors. The initial and maximum Young's modulus E_{max} of 180 MPa appears in good agreement with the expected value for this sand, density and stress condition (Cazacliu, 1996).

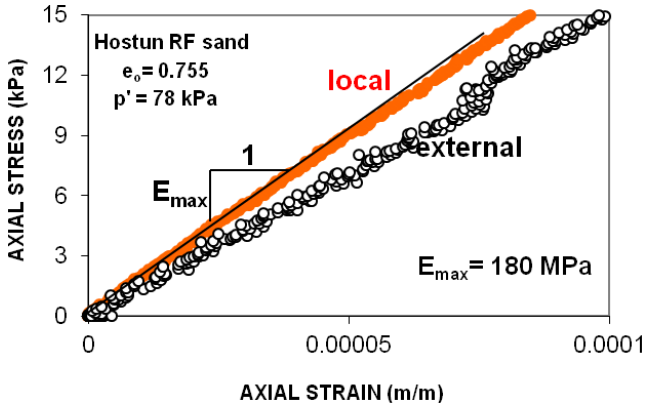

Figure 8 Initial deviator stress–strain response of dry sand in triaxial compression: local and external axial strain measurements.

A second series of tests has been performed on saturated samples. The saturation procedure followed the usual combination of CO_2/de-aired water flushing and back-pressure application. The local measurement systems were tested for samples loaded in isotropic conditions but also in triaxial compression loading. The inner and outer cell pressures were kept equal throughout the tests so that the circumferential stress was always equal to the radial stress. Two typical tests and subsequent results are presented in this paper.

A sand specimen (fabrication void ratio e_o = 0.756) was initially subjected to an isotropic consolidation up to a mean effective pressure, p', of 300 kPa (Figure 9). The performance of the loading and measurement systems to provide access to the elastic properties of the sand material was assessed at different stress investigation points (1 to 5, Figure 9), approximately every 50 kPa by application of successive and independent small cyclic loadings in vertical and torsional directions. Different cyclic amplitudes and loading frequencies have been employed.

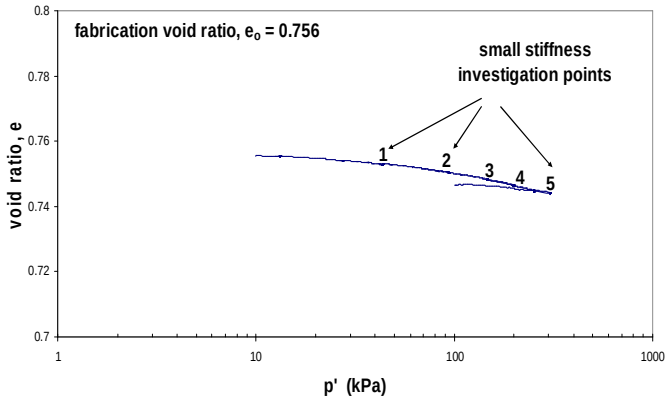

Figure 9 Mean effective stress (p') - void ratio (e) relationship during isotropic consolidation.

Figure 10 shows the time history of the axial and shear stresses applied to the sample at an investigation point p'=95 kPa. Small load/unload cycles of magnitudes up to ±6 kPa in vertical direction and ±3 kPa in torsional direction were applied at different time intervals. During these cycles only one stress component was changed at a time and it can be observed that during the torsional cycles the hydraulic system effectively maintains the constant axial load (Figure 10).

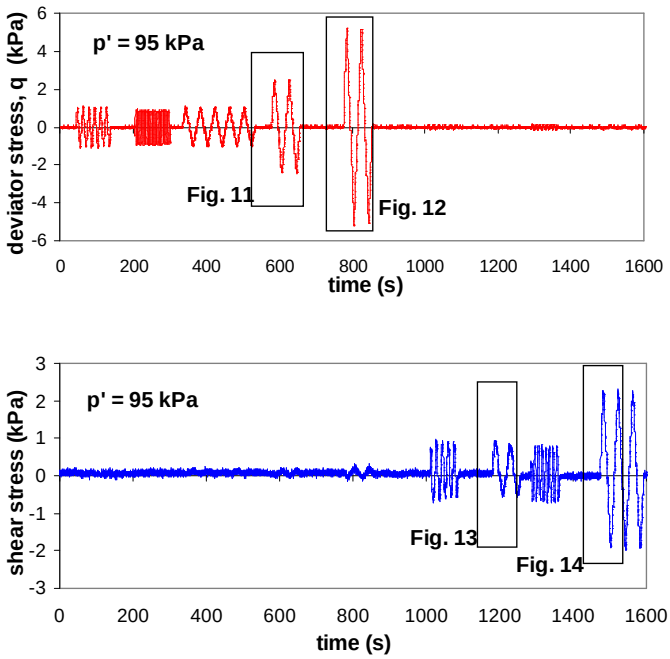

Figure 10 Time history of the axial (red) and shear (blue) stress cycles at an investigation point p'=95 kPa with small load/unload cycles of magnitudes up to ±6 kPa in vertical direction and ±3 kPa in torsional direction.

The quality of the axial and torsional cyclic loadings has been assessed against different loading frequencies of 0.0625Hz, 0.25Hz, 0.025Hz for axial direction and 0.065Hz, 0.025Hz and 0.1Hz for torsional direction. For the amplitudes of cyclic loading employed, and for both axial and torsional directions, it was observed that the best control of the cyclic load is obtained for a frequency of 0.025Hz. Two pairs of small load/unload axial and torsional cycles performed at this frequency have been isolated and presented together with the recorded corresponding strain responses in the Figures 11-14. As can be observed from these figures, the start of the loading is very smooth and the loading rate for all the selected cases appears constant with no backlash or time lag on the reversal of the load with just one exception, when the torsional cyclic stress level is very low, up to ±1 kPa (Figure 13). The axial and shear strain responses recorded with the local measurement systems are also presented in Figures 11-14. The axial and shear strains show an excellent repeatability of the responses for these successive cycles. The double amplitude of the cyclic axial strain response reaches $2x10^{-5}$ for ±2.5 kPa cyclic axial stress amplitude (Figure 11) and $4.3x10^{-5}$ for ±5.5 kPa cyclic axial stress amplitude (Figure 12). For each axial cyclic loading, the superposition of the stress-strain relations is identical and linear with no hysteresis or energy dissipation. It can also be observed from Figures 11 and 12 that the equivalent vertical Young's modulus, E_z, calculated from inclination of stress-strain response is nearly the same for both cyclic amplitude levels. Similar observations can be made on the shear stress-strain probing shown in Figures 13 and 14. The double amplitude of the cyclic shear strain response reaches $1.5x10^{-5}$ for ±1.0 kPa cyclic shear stress amplitude (Figure 13) and $4.3x10^{-5}$ for ±2.5 kPa cyclic shear stress amplitude (Figure 14).

Figures 15 and 16 show some typical small load/unload cycles applied in axial and torsional directions, respectively, at some different confining pressures. The Young's, E_z, and shear, $G_{z\theta}$, moduli were calculated from the slopes, as shown in the figures. One can comment on the quality of the recorded strain responses by the local measurement systems which are able to identify the behaviour for small double amplitudes of cyclic strain with the order of $0.65x10^{-5}$ for axial direction and $1.2x10^{-5}$ for torsional direction.

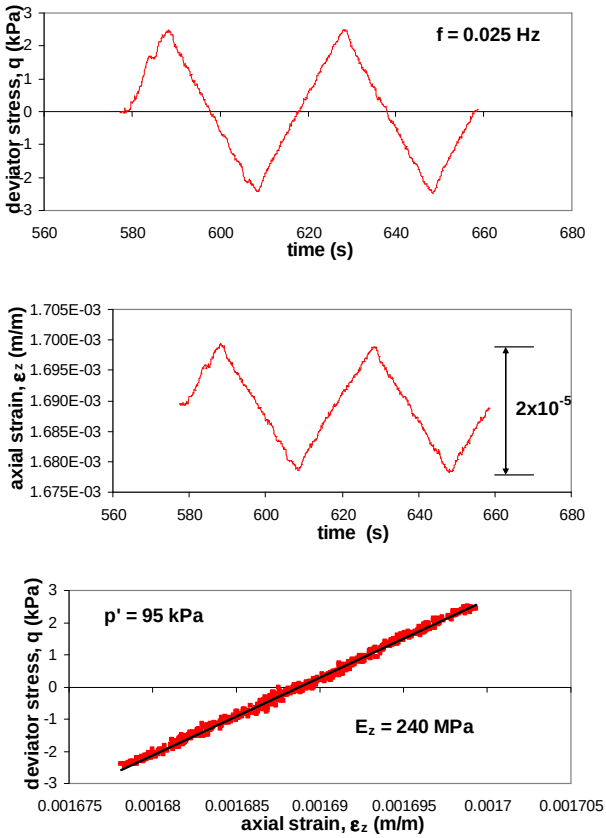

Figure 11 Two successive load/unload axial cycles of ±2.5 kPa stress amplitude, axial strain response with time and the corresponding stress-strain relationship

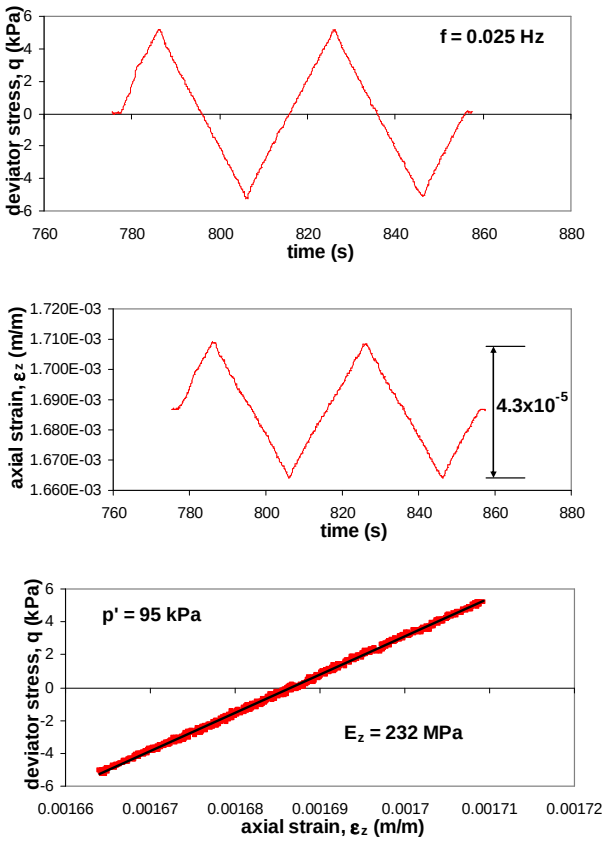

Figure 12 Two successive load/unload axial cycles of ±4.5 kPa stress amplitude, axial strain response with time and the corresponding stress-strain relationship

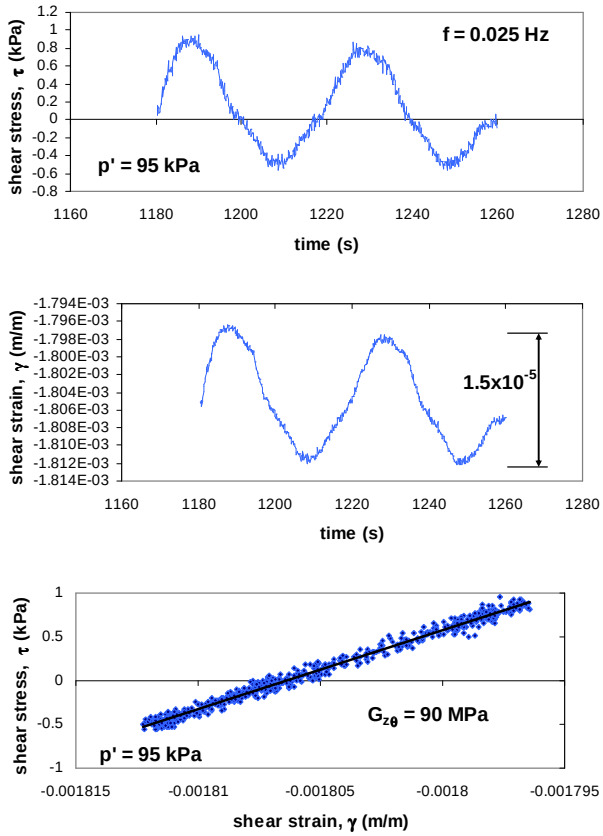

Figure 13 Two successive load/unload torsional cycles of ±1.0 kPa stress amplitude, shear strain response with time and the corresponding stress-strain relationship

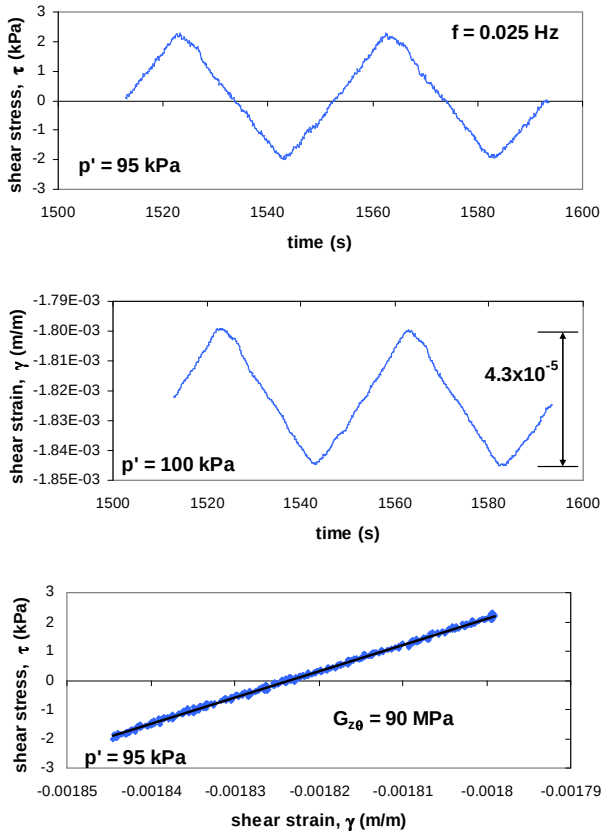

Figure 14 Two successive load/unload shear cycles of ±2.5 kPa stress amplitude, shear strain response with time and the corresponding stress-strain relationship

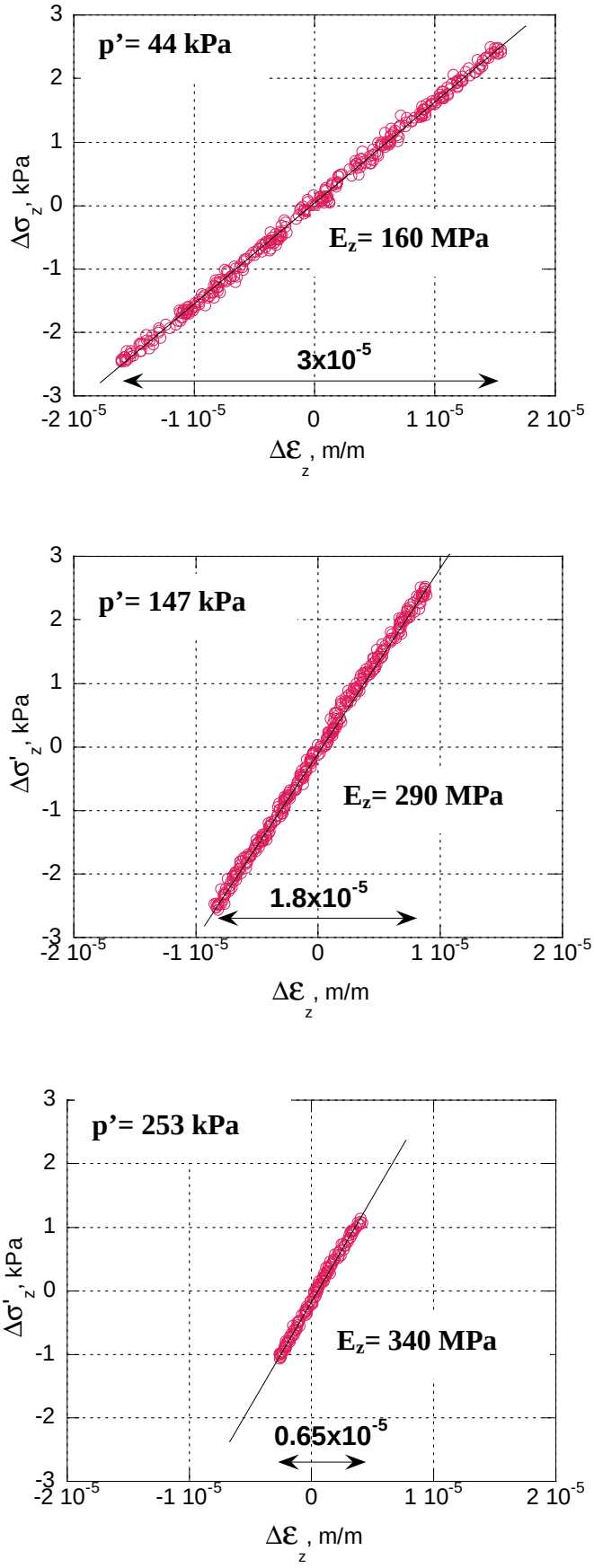

Figure 15 Typical small load/unload axial cycles at different investigation points during the isotropic consolidation.

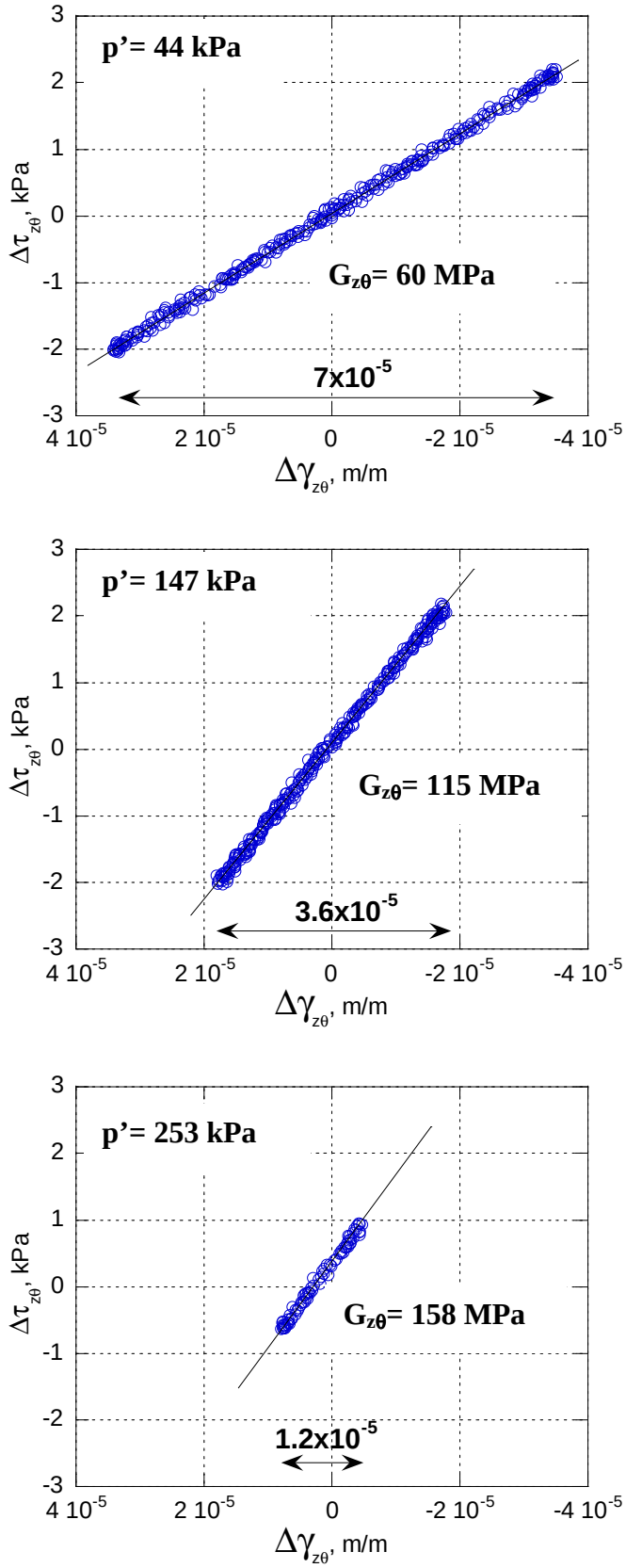

Figure 16 Typical small load/unload shear cycles at different investigation points during the isotropic consolidation.

It is already established that the elastic Young's modulus is dependent on the normal stress in the direction of measurement following a power law (Hardin and Blandford, 1989, Tatsuoka et al., 1999). The density of soil also affects the stiffness and its influence is normally taken into account by the use of a void ratio function, F(e). Based on a large experimental data obtained from resonant column tests, shear wave propagation and local strain measurements, Hameury (1995) proposed the following expression of the void ratio function for the Hostun RF sand:

$$F(e) = \frac{(3.01-e)^2}{1+e} \qquad (2)$$

It is also recognised that the shear modulus is mainly dependent on the two normal stresses acting on the plane of shear and independent of the stress acting normal (Roesler, 1979).

Figure 17 shows the pressure dependency of shear and Young's moduli obtained from the isotropic compression test. The effect of the void ratio variation is removed by normalising the E_z and $G_{z\theta}$ values by the void ratio function (2). It can be observed that on the full logarithmic plot both moduli increase almost linearly with the mean effective stress, p' (for isotropic consolidation, $\sigma_z = \sigma'_\theta = p'$). Therefore, $E_z/f(e)$ and $G_{z\theta}/f(e)$ can both be modelled as a function of p'^m with constant power values *m* of 0.43 and 0.54 respectively. These exponent values are within the expected values for sand and close to those obtained by Cazacliu (1998) and Hameury (1995). In the equations presented in the Figure 17, p_r represents a reference pressure of 1 kPa.

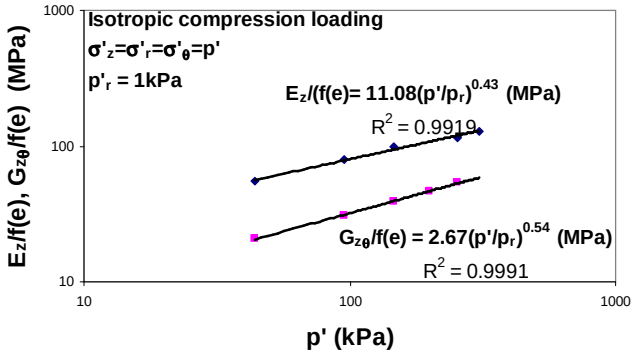

Figure 17 Pressure dependencies of E_z and $G_{z\theta}$ moduli in isotropic compression loading.

The Poisson's ratio, $\nu_{z\theta}$, was calculated by linear regression analysis through the unload/reload response of axial, ε_z, and circumferential, ε_θ, strains at different consolidation pressures, as shown as an example in Figure 18. The calculation of the circumferential strain is based only on the outer radius variation obtained through the use of the non-contact measurement system. The Poisson's ratios, $\nu_{z\theta}$, seem to be independent of the mean effective pressure, p' (Figure 19). The average value of $\nu_{z\theta}$ for the confining pressures employed in this study is around 0.24 which is again in accord with Cazacliu and Di Benedetto (1998).

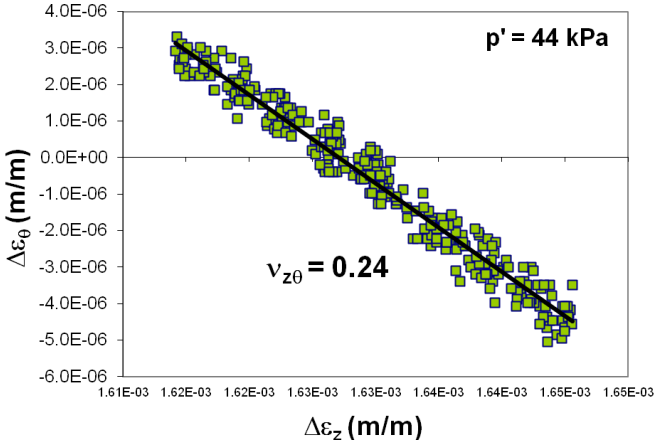

Figure 18 Typical determination of the Poisson ratio, $\nu_{z\theta}$ at a confining pressure of 44kPa

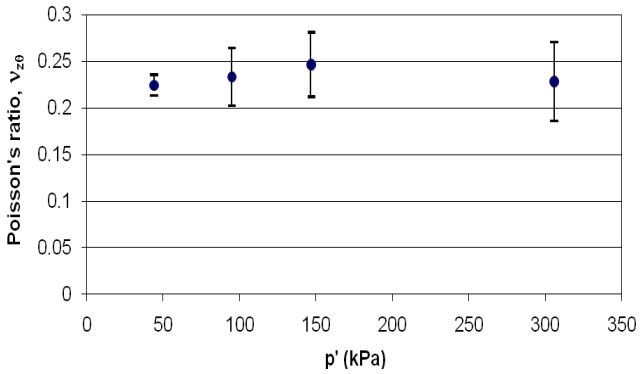

Figure 19 Poisson ratio, $\nu_{z\theta}$ during isotropic consolidation

Once the effective mean pressure, p', reached 300 kPa, the isotropic confining pressure was reduced to 100 kPa and the specimen was subjected to a drained triaxial compression test up to a deviator stress, $q = \sigma'_z - \sigma'_\theta$, of 141 kPa, corresponding to approximate 25° mobilised angle of friction. The initial deviator stress-axial strain responses recorded by the local measurement system as well as by the external LVDTs are shown in the Figure 20. As expected, the stiffness recorded by the local measurement system is higher than the stiffness given by the external one. The slope of the initial part of the stress-strain curve gives an initial stiffness of 225 MPa. The evolution of the secant Young's modulus with the strain level up to 10^{-4} m/m is presented in Figure 21. In spite of some scatter of data observed for axial strains below 3×10^{-6} m/m, the stiffness of the sand appears to exhibit a plateau at strain levels up to 2×10^{-5} m/m (around 225 MPa).

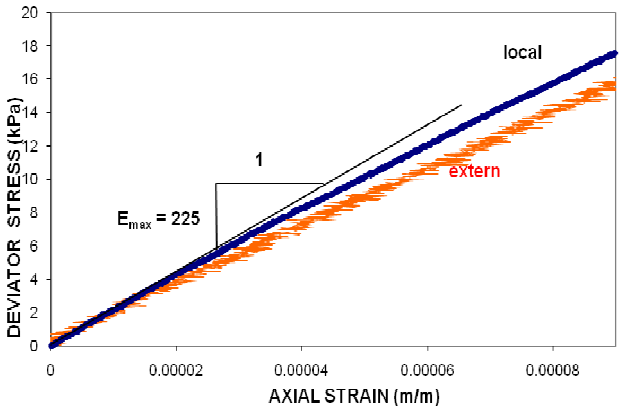

Figure 20 Initial deviator stress–axial strain response in triaxial compression: local and external axial strain measurements.

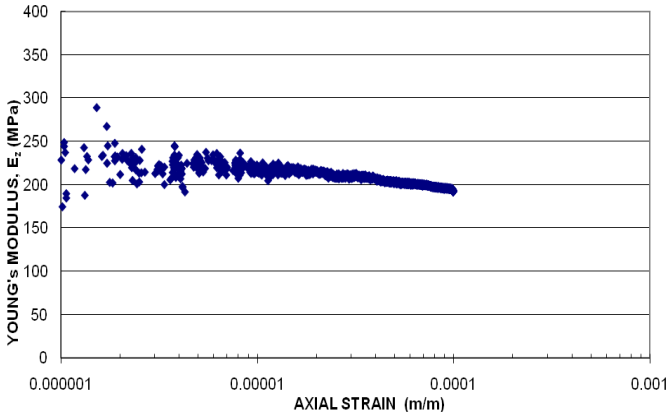

Figure 21 Axial Young's modulus variation with local axial strains up to 10^{-4} m/m in triaxial compression loading

At different deviator stresses (investigation points) and after creep periods up to 40 minutes, several small unload/reload cycles were also applied in the vertical and torsional directions. During the axial cyclic loading, the axial stress was varied at constant confining stress (and with no shear stress), while the torsional shear loading was applied at constant axial and confining stresses. Figures 22 and 23 show some typical small cycle responses in axial and torsional directions, respectively. In general, the level of the applied cyclic stress amplitude was relatively low and this affected in some way the quality of the measurements especially for the torsional direction. However, the moduli measured by linear regression followed almost the same power laws as in the case of isotropic compression loading. The Young's modulus values normalised with the void ratio function could be represented as a function of σ'^{m}_z with a power value of 0.41, closer to m=0.44 obtained for the isotropic compression, Figure 24. The normalised shear modulus could also be modelled by a function of the product $(\sigma'^{m1}_z \sigma'^{m2}_q)$, and since in triaxial compression σ'_z and σ'_θ are not equal, the power exponents can be estimated by linear regression as shown in Figure 25. While m_1=0.39 and m_2=0.20, their sum is also closer to the value of the power exponent of 0.54 previously obtained on isotropic stress states.

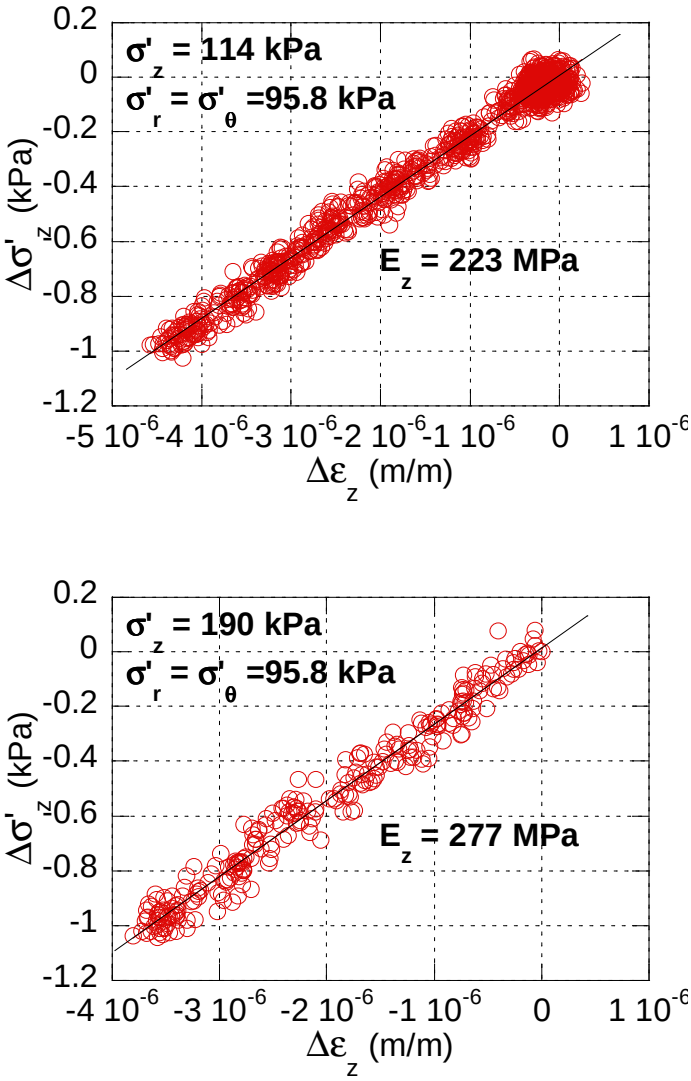

Figure 22 Typical small unload/reload axial cycles at different investigation points during the triaxial compression test

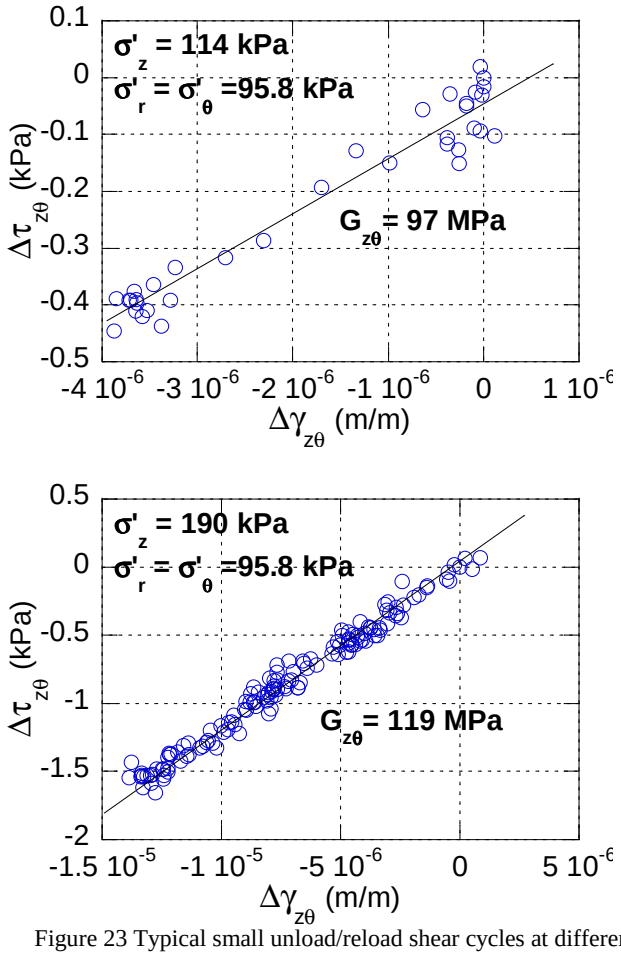

Figure 23 Typical small unload/reload shear cycles at different investigation points during the triaxial compression test

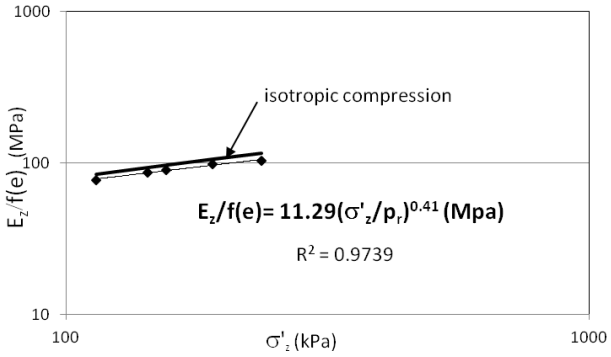

Figure 24 Stress dependency of E_z in triaxial compression

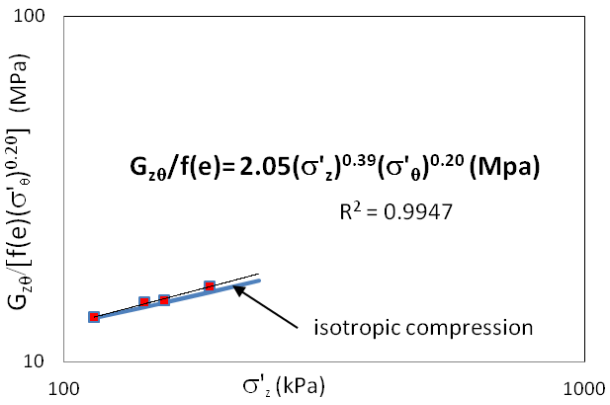

Figure 25 Stress dependency of $G_{z\theta}$ in triaxial compression

5. CONCLUSION

A hollow cylindrical torsional apparatus (HCTA) was recently developed at University of Bristol, UK. The HCTA apparatus is designed for testing granular soils in drained and undrained, in monotonic but also dynamic loading conditions, and it is equipped with a complex strain measurement system based on high resolution non-contact transducers. The experimental developments are designed to allow the study of the pre-failure deformation characteristics and the large strains behaviour, via a continuous test on a single specimen and, thus, analyse the soil stiffness with the evolution of the strain and stress levels. This paper focuses mainly on the precision measurement system and includes the assessment of its performance with reference to the soil stiffness recorded during isotropic and triaxial compression loadings. Only the Young's modulus and the shear modulus have been considered so far. The results show that the new local measurement system is performing well over the range of the stresses employed; power laws of stiffness moduli with the normal stresses as typically observed for sand materials have been obtained. The next stage of the experimental development nevertheless should involve improvements of the sample radial measurements (inner radius) as currently the radial strain cannot provide the required precision for small strain domain.

AKNOWLEDGMENTS

This work was financially supported by an EPSRC research grant (GR/R57645/01). The commissioning of the hydraulic loading system was completed with the support of a JIF research project Bristol Laboratory for Advanced Dynamics Engineering (BLADE).

6. REFERENCES

Arroyo, M., Muir Wood, D., Greening, P. Medina, L. and Rio, J. (2006) "Effects of sample size on bender-based axial G_0 measurements". Géotechnique, 56(1), pp39-52.

Arthur, J. R. F., Chua, K. S., Dunstan, T. and Rodriguez del C., J. I. (1980) "Principal stress rotation: a missing parameter". Journal of the Geotechnical Engineering Division, Proceedings of the ASTM, Vol. 106, No. GT4, pp419-433.

Baldi, G., Hight,D.W., and Thomas, G. E., (1988) "A Re-Evaluation of Conventional Triaxial Test Methods" Advanced Triaxial Testing of Soil and Rock, ASTM STP 977, ASTM International,West Conshohocken, PA, pp 219–263.

Bellotti, R., Jamiolkowski, M., Lo Presti, D.C.F., O'Neil, D.A. (1996) "Anisotropy of small strain stiffness in Ticino sand". Géotechnique, 46, N° 1, pp115-131.

Boung Shik, Y. (2005) "Commissioning of a new hollow cylinder apparatus" MSc Thesis, University of Bristol, UK

Brignoli, E.G.M., Gotti M. and Stkoe, J.H. (1996) "Measurement of shear waves in laboratory specimens by means of piezoelectric transducers". Geotechnical Testing Journal, 19, pp284-397

Cazacliu, B. (1996) "Comportement des sables en petites et moyennes deformations: prototype d'essai de torsion compression confinement sur cylinder creux", PhD Thesis, ECP/ENTPE, France, p241.

Cazacliu, B. and Di Benedetto, H. (1998) "Behavior of Sand in the Small Strain Domain Observed with a Hollow Cylinder Apparatus". Proceedings of 11thECEE, CD-ROM, Balkema, Rotterdam, p10.

Chaudhary, S.K., Kuwano, J., Hayano, Y. (2004) "Measurement of quasy-elastic stiffness parameters of dense Toyoura sand in Hollow Cylinder Apparatus and Triaxial Apparatus with bender elements" Geotechnical Testing Journal 27(1), pp1-13.

Christiaens, P. (2006) "Small strains in Hollow Cylinder Torsional Shear Apparatus". Research project TFE, University of Bristol, p79.

Connolly, T.M. and Kuwano, R. (1999) "The measurement of G_{max} in a resonant column, bender element, torsional shear

apparatus", Proc. of 2nd Int. Symp. on Pre-failure Def. Charact. of Geomaterials, Torino, pp89-96.

Clayton, C.R.I. (2010) "Stiffness at small strain: research and practice". Géotechnique, 61, No. 1, pp5-37.

Clayton, C. R. I., Priest; J. A., Bui; M., Zervos; A. and Kim, S. G. (2009) "The Stokoe resonant column apparatus: effects of stiffness, mass and specimen fixity" Géotechnique, 59 (5), pp 429–437

Clayton, C.R.I. and Heymann, G. (2001) "Stiffness of geomaterials at very small strains". Géotechnique, 51, pp245-255.

Duttine, A; Di Benedetto, H; Van Bang, DP, Ezaoui, A. (2007) "Anisotropic small strain elastic properties of sands and mixture of sand-clay measured by dynamic and static methods". Soils and Foundations, Vol. 47, Issue 3, pp457-472.

Di Benedetto, H., Cazacliu, B., Geoffroy, H. And Sauzeat, C. (1999) "Sand behaviour in very small to medium strain domains", Proc. of 2nd IS on Pre-failure Deformation Characteristics of Geomaterials, Torino, pp89-96.

Di Benedetto, H., Geoffroy, H., and Sauzeat, C. (2001) "Viscous and non viscous behaviour of sand obtained from hollow cylinder tests", in Advanced laboratory stress-strain testing of geomaterials (eds Tatsuoka, Shibuya, Kuwano), pp217-226.

Dyvik, R. and Madshus, C. (1985) "Laboratory measurements of G_{max} using bender elements". Proc. ASCE Annual Convention: Advances in the art of testing soils under cyclic conditions, Detroit, Michigan, pp186-197.

Fioravante, V (2000) "Anisotropy of small strain stiffness of Ticino and Kenia sands from seismic wave propagation measured in triaxial testing". Soils and Foundations, 40(4), pp129-142.

Geoffroy, H., Di Benedetto, H., Duttine, A., and Sauzeat, C. (2003) "Dynamic and cyclic loadings on sand: results and modeling for general stress-strain conditions". Proc. of 3rd IS on Pre-failure Deformation Characteristics of Geomaterials, Lyon, Vol. I, pp353-363.

Hameury, O. (1995). "Quelques aspects du comportement des sables avec ou sand rotation des axes principauxx des petites aux grandes deformations". PhD Thesis, ECP/ENTE France.

Hardin, B.O., and Richart, F.E.Jr. (1963) "Elastic wave velocities in granular soils". Journal of the Soil Mechanics and Foundations Division, ASCE, Vol. 89, SM1, pp33-65.

Hardin, B.O. and Black, W.L. (1966) "Sand stiffness under various triaxial Stresses". Journal of Soil Mechanics and Foundation Division, ASCE, SM2, pp27-42.

Hardin, B. O. and Blandford, G. E. (1989) "Elasticity of Particulate Materials". Journal of Geotechnical Engineering, American Society of Civil Engineers, Vol. 115, No. 6, pp788–805.

Hight, D.W., Gens, A., and Symes, M.J. (1983) "The development of a new hollow cylinder apparatus for investigating the effects of principal stress rotation in soils". Géotechnique, 33, N° 4, pp355-383.

HongNam, N. and Koseki, J. (2005) "Quasy-elastic deformation properties of Toyoura sand in cyclic triaxial and torsional loadings". Soils and Foundations, 45(5), pp19-38.

Ibraim, E. (1993) "Comportement du sable à l'aide d'essais sur cylindre creux: observations expérimentales et conditions d'utilisation des capteurs sans contact". MSc Thesis (DEA) ENTPE-INSA-ECL-UL

Jardine, R.J., Symes, M.J. and Burland, J.B. (1984) "The measurement of soil stiffness in the triaxial apparatus". Géotechnique, 34, N° 3, pp323-340.

Jardine, R.J., Potts, D.M., Fourie, A.B. and Burland, J..B. (1986) "Studies of the influence of non-linear characteristics in soil-structure interaction" Géotechnique, 36, N° 3, p. 377-396.

Jardine, R.J. (1992) "Some observations on the kinematic nature of soil stiffness" Soils and Foundations , 32(1), p111-124.

Kuwano, R. and Jardine, R.J. (2002) "On the applicability of cross-anisotropic elasticity to granular materials at very small straains", Géotechnique, 52, N° 10, pp727-749.

Lings, M., Pennington, D.S., and Nash, D.F.T. (2000) "Anisotropic stiffness parameters and their measurement in a stiff natural clay", Géotechnique, Vol. 50, N° 2, pp109-125.

Lo Presti, D.C.F., Pallara, O., Lancellotta, R., Armandi, M., and Maniscalco, R. (1993) "Monotonic and cyclic loading behaviour of two sands at small strains". Geotechnical Testing Journal, Vol. 16, N° 4, pp409-424

Lo Presti, D.C.F., Jamiolkowski, M., Pallara, O., Cavallaro, A., and Pedroni, S. (1997) "Shear modulus and damping of soils". Géotechnique, 47, pp603-617.

O'Kelly, B.C. and Naughton, P.J. (2005) "Development of a new hollow cylinder apparatus for stress path measurements over a wide strain range". Geotechnical Testing Journal, Vol. 28, No. 4, , pp345-354.

Palomero, J.V.H. (2002) "New hollow cylinder torsional apparatus". Research project, University of Bristol, p44.

Pennington, D.S., Nash, D.F.T., and Lings,M.L., (1997) "Anistropy of G_0 Shear Stiffness in Gault Clay". Géotechnique, Vol. 47, No. 3, pp391–398.

Roesler (1979) "Anisotropic shear modulus due to stress anisotropy" J Geot Eng, ASCE 105(GT7), pp 871-880.

Sayao, A. and Vaid, Y.P. (1991) "A critical assessment of stress non-uniformities in hollow cylinder test specimens". Soils and Foundations, Vol. 32, No. 1, pp60-72.

Shirley, D. J., and Hampton, L. D. (1978) "Shear-Wave Measurementsin Laboratory Sediments". Journal of the Acoustical Society of America, Vol. 63, No. 2, pp607–613.

Schultheiss, P.J. (1980) "Simultaneous measurement of P and S wave velocities during conventional laboratory soil testing procedures" Marine Geotechnology, Vol 4, no 4, pp343-367

Simpson, B., Atkinson, J.H. and Jovicic (1996) "The influence of anisotropy on calculations of ground settlements above tunnels." Geotechnical aspects of underground construction in soft ground (ed RN Taylor), pp591-595.Th. Telford Ed.

Shibuya S., Tatsuoka F., Teachavorasinskun S., Kong, X.J., Abe, F., Kim, Y-S., and Park, C-S. (1992) "Elastic deformation properties of geomaterials". Soils and Foundations, Vol. 32, no.3, pp26-46.

Tatsuoka, F., Sato, T., Park, C.-S., Kim, Y.-S., Mukabi, J. N., and Kohata, Y. (1994) "Measurement of Elastic Properties of Geomaterials in Laboratory Compression Tests". Geotechnical Testing Journal, Vol. 17, No. 1, pp80–94.

Tatsuoka, F., Jardine, R. J., Lo Presti, D. C. F., Di Benedetto, H., and Kodaka, T. (1998) "Characterising the Pre-Failure Deformation Properties of Geomaterials". Theme lecture, Plenary Session 1, Proceedings XIV ICSMFE, Hamburg, Balkema, Vol. 4, pp2129–2164.

Tatsuoka, F. and Shibuya, S. (1992) "Deformation and characteristics of soils and rocks from field and laboratory tests". Keynote lecture, Proc. of 9th Asian regional Conf. on SMFE, Bangkok, Vol. 2, pp101-170

Tatsuoka, F., Modoni, G., Jiang, G. L., Anh Dan, L. Q., Flora, A., Matsushita, M., and Koseki, J. (1999) "Stress-Strain Behaviour at Small Strains of Unbound Granular Materials and its Laboratory Tests" Keynote Lecture, Proceedings, Workshop on Modelling and Advanced Testing for Unbound Granular Materials, Eds., Balkema, pp17–61.

Viggiani, G. and Atkinson, J. H. (1995) "Interpretation of Bender Element Tests". Géotechnique, Vol. 45, No. 1, pp149–154.

Yamashita, S., Kawaguchi, T., Nakata, Y., Mikami, T., Fujiwara, T. and Shibuya, S. (2009) "Interpretation of international parallel test on the measurement of G_{max} using bender elements" Soils and foundations, 49(4), pp631-650.

Zdravkovic, L. and Jardine, R.J. (1997) "Some anisotropic stiffness characteristics of a silt under general stress conditions". Géotechnique, 47, N° 3, pp407-437.